Structural and Magnetic Properties of Nickel Spinel Doping Gadolinium Synthesized by using Citrate Precursor Technique

Luong Ngoc Anh*, To Thanh Loan

Hanoi University of Science and Technology, No. 1, Dai Co Viet, Hai Ba Trung, Hanoi, Viet Nam

Received: March 21, 2017; accepted: June 9, 2017

Abstract

$NiGd_{0.1}Fe_{1.9}O_4$ nanoparticles have been synthesized by citrate precursor technique and annealed at 700° C in 5 h. Indexed X-ray diffraction (XRD) patterns analysised by Rietveld method, scanning electron microscopy (SEM) and integrals magnetometer (IM) are utilized in order to study the effect of gadolinium substitutions and its impact on crystalline size, lattice parameter, cation distribution, microstructure and magnetic properties of the $NiFe_2O_4$ and $NiGd_{0.1}Fe_{1.9}O_4$ samples. Results have shown that the formation of pure cubic spinel phase, the lattice parameter a increases and crystallite size D decreases with on Gd^{3+} substitution. SEM images show that the particle samples have spherical morphology and uniform size distribution. Magnetization as a function of temperature was determined via magnetization curves measured by integrals magnetometer in temperature range from 88 K to above Curie temperature in applied fields up to 10 kOe. The spontaneous magnetization M_{sp} and Curie temperature of the samples were determined and discussed based on the influences of the particles size, cation distribution and gadolinium substitution effects.

Keywords: Nanoparticles, Ni ferrite, Cation distribution, Sol-gel method.

1. Introduction

Spinel ferrites are a class of magnetic materials with ferric ions as the main component having formula MFe_2O_4, where M is divalent metal ion such as Mn^{2+}, Ni^{2+}, Zn^{2+}, Cd^{2+}, Mg^{2+}, Fe^{2+}, and so on. By mixing two or more kinds of M^{2+} ions, one can formulate mixed ferrites to modify its physical properties according to the required applications. That is why they are extensively used as core materials for inductances and transformers in telecommunication industry, audio and video recording heads, memory devices, digital systems, tapes, magnetic memory and spintronic devices, and so on [1]. $NiFe_2O_4$ compound crystallizes in inverse spinel cubic structure [2]. In this structure the tetrahedral site (A site) is fully occupied by Fe^{3+} while the octahedral site (B site) is occupied by Ni^{2+} and Fe^{3+} ions [3]. Substitution of trivalent rare earth ions in nickel ferrite may influence the magnetic, structural and electric properties which make it more suitable for transmission of high frequency microwaves and its use in magneto-optic recording devices, etc. [4]. Bharathi and Markandeyulu have studied the electrical and magnetic properties of *RE*-doped nickel ferrite at room temperature [5]. The effect of *RE* substitution on the magnetostrictive properties of nickel ferrite at 80 K and 300 K has been reported by Bharathi et al.[6]. Structural, magnetic, electric and optical properties of $NiGd_{0.04}Fe_{1.96}O_4$ nanoparticles have been studied by Singh et al. [7]. Electrical and magnetic properties have been investigated for the use of nickel holmium ferrites in high frequency devices especially for electromagnetic interference suppression and microwaves absorbing material [8]. Recently, Dixit et al. [9] have investigated the swift heavy ion-induced effects in nanoparticles of Ce-doped nickel ferrite. To the best of our knowledge, change in spin and orbital moments on doping of Gd in nickel ferrite which may decide their intriguing magnetic properties is still unexplored. Therefore, it was thought of interest to investigate the temperature dependent (80 K to above Currie temperature) spin momentum densities of $NiGd_{0.1}Fe_{1.9}O_4$. In this report, we have substituted Gd atoms in $NiFe_2O_4$ in order to induce grain size reduction and their cation distributions. The variations of magnetic properties as a function of size of the nanoparticles have been investigated.

2. Experimental

$NiFe_2O_4$ and $NiGd_{0.1}Fe_{1.9}O_4$ nanoparticles in the present study were synthesized a modified citrate precursor technique. All the chemicals purchased were of analytical grade and used as received. Aqueous solutions of Iron nitrate $Fe(NO_3)_3$, $Gd(NO_3)_3$ and $Ni(NO_3)_2$ were prepared by dissolving stoichiometric amounts of nitrate salts in deionized water. Amounts of $Ni(NO_3)_2$, $Gd(NO_3)_3$ and $Fe(NO_3)_3$ with molar ratios $[Ni^{2+}]:[Gd^{3+}]:[Fe^{3+}]$ = 1:0.1:1.9 were dissolved completely in deionized

Corresponding author: Tel.: (+84) 904.147.046
Email: ngocanh@itims.edu.vn

water. Molar ratio of M^{3+} and M^{2+} were kept 2:1. Aqueous nitrates were then mixed with a magnetic stirrer. Aqueous solution of citric acid were prepared with the ratio of Citric acid/Nitrates = 1/2 and mixed with the nitrate solution. The mixed solution was magnetically stirred for 1 h. The solution were then neutralized with aqueous ammonia and heated at 90°C till the liquid turns to a gel. Gel then automatically converted to fluffy powders by self ignition. Prepared powders were then dried further in an electric oven at 130° C for 24 h and then heated in air at 350° C for 2 h in order to form xerogels. The nanoparticle samples were obtained after sintering the products in a muffle furnace for further characterizations at 700° C in 5h.

X-ray diffraction (Cu–Kα, Siemens D–5000) was employed to identify the crystal structure of the samples at room temperature. Scanning Electron Microscopy (JSM 7600F) was used to examine the particle size and morphology. Infrared (IR) absorption spectra of the samples were recorded on Perkin Elemer FT–IR spectrum one spectrometer in the frequency range 400–2000 cm^{-1}. Magnetization curves were measured using a integrals magnetometer in applied magnetic fields up to 10 kOe and at temperatures from 87 K to well above the Curie temperature.

3. Results and disscution

X-ray powder diffraction (SXRD) experiment was carried out using Siemens D5000 X-ray diffractometer (CuKα radiation, λ = 1.54056 Å) to identify the crystal structure of the sample at room temperature. The data were processed to analyze using the Rietveld method with the help of FullProf program [10]. The diffraction peaks were modeled by pseudo-Voight function. The refinement fitting quality was checked by goodnessof fit (χ^2) and weighted profile *R*-factor (R_{wp}) [11].

Fig. 1 shows the XRD patterns of the sample refined using FullProf program. All the diffraction peaks correspond to the cubic spinel structure, which confirm the formation of phase-pure spinel ferrite in the sample. The structural parameters of the sample were well refined via Rietveld analysis using the standard model of spinel ferrite within the cubic symmetry (space group *Fd3m*) with atoms in positions A-site in *8a*(1/8, 1/8, 1/8), B-site in *16d*(1/2, 1/2, 1/2) and O in *32e*(*u*, *u*, *u*). The refined values of structural parameters are as follows: lattice constant *a* = 8.3384 ± 0.0011 (Å) and oxygen positional parameter *u* = 0.2555 ± 0.0009. Lattice constant of the sample is slightly larger than that of undoped $NiFe_2O_4$ prepared by using the same conditions (Table 1), which can be explained due to the larger ionic radii of Gd^{3+} ion compared to that of Fe^{3+} ion (r_{Gd}^{3+} = 1.078Å and r_{Fe}^{3+} = 0.785 Å). The obtained value of oxygen positional parameter is characteristic of the spinel-type structure [12]. The average size of coherent scattering region *D* (usually called the crystallite size) was obtained by analysis of the peak broadening on applying Rietveld method using FullProf. Crystallite size of the sample was obtained to be *D* = 9.3 ± 0.1 (nm), which is smaller than crystallite size of nickel ferrite prepared by using the same method (Table 1). The cation distribution of the sample was also refined via Rietveld analysis. The result indicated that Ni^{2+} ion occupies both A and B sites, whereas Gd ion occupies only B site. And then the formula of the sample can be written as $(Ni_{0.03}Fe_{0.97})^A[Ni_{0.97}Fe_{0.93}Gd_{0.1}]^BO_4$ (Table 1.).

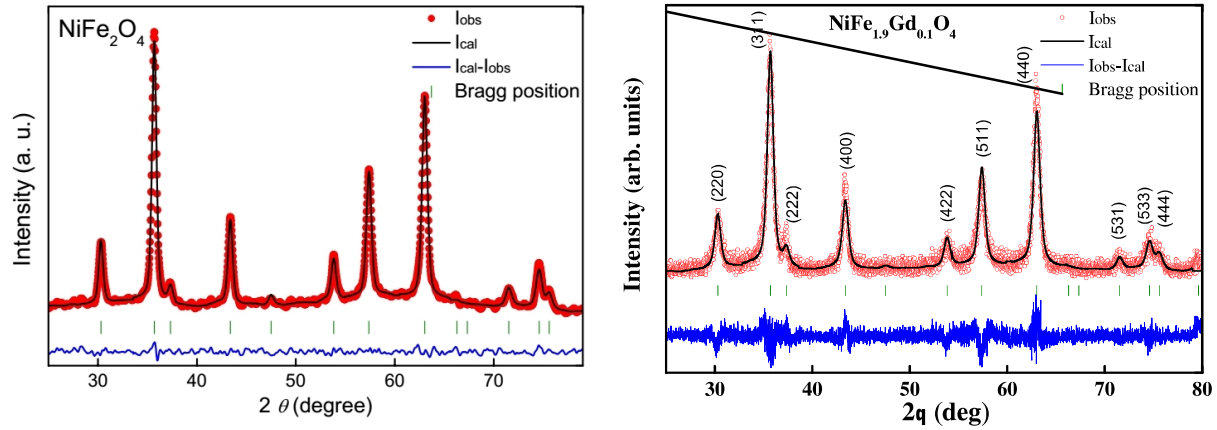

Fig. 1. The Rietveld refinement pattern and diffraction plot of x-ray diffraction data of the $NiFe_2O_4$ (a) and $NiGd_{0.1}Fe_{1.9}O_4$ (b) samples annealed at 700° C in 5h. The experimental points as well as calculated and difference functions are indicated.

Table 1. Result obtained from XRD analysis. Lattice parameter a, unit cell volume V, coordinate of oxygen x(O), average crystallite size D_{XRD}, cation distribution in A and B sites and the refinement fitting quality of the samples $NiFe_2O_4$ and $NiGd_{0.1}Fe_{1.9}O_4$.

Sample	$NiFe_2O_4$	$NiGd_{0.1}Fe_{1.9}O_4$
A (Å)	8.3323	8.3384
V (Å^3)	578.49	579.76
D_{XRD} (nm)	17.2	9.3
x(O)	0.2567	0.2555
A–*site*	$Ni_{0.1}Fe_{0.9}$	$Ni_{0.03}Fe_{0.97}$
B–*site*	$Ni_{0.9}Fe_{1.1}$	$Ni_{0.97}Gd_{0.1}Fe_{0.93}$
R_{wp} (%)	11.7	12.8
χ^2	1.55	1.43

Morphology of the prepared $NiFe_2O_4$ and $NiGd_{0.1}Fe_{1.9}O_4$ nanoferrites were observed by SEM. Fig. 2 shows the electron microscopy images for the samples (a) $NiFe_2O_4$ and (b) $NiGd_{0.1}Fe_{1.9}O_4$. It is obvious from the micrograph that spherical uniform and homogenous nanoparticles have been prepared by citrate precursor technique along with a narrow size distribution and less agglomeration. Variation of porosity can be observed from the comparison of the images for $NiFe_2O_4$ and $NiGd_{0.1}Fe_{1.9}O_4$ where it decreases with substituted in the concentration of Gd^{3+} ions. Average particle size was observed in the range of 10 nm to 22 nm.

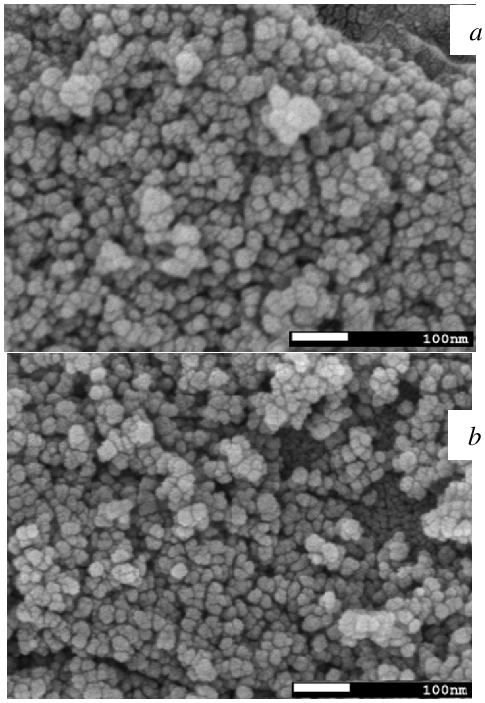

Fig. 2. SEM images of (a) $NiFe_2O_4$ and (b) $NiGd_{0.1}Fe_{1.9}O_4$ samples annealed at 700° C in 5h

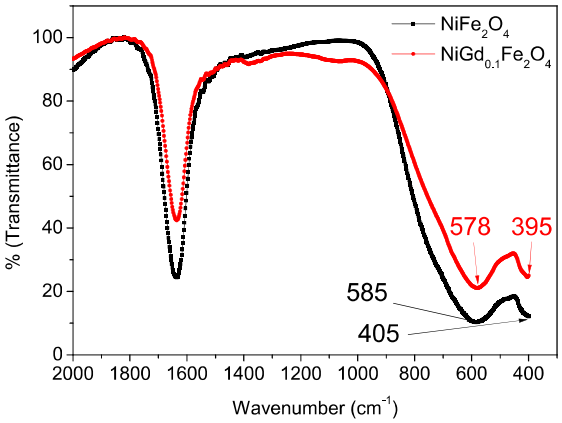

Fig. 3. FT-IR absorption spectra of the samples $NiFe_2O_4$ and $NiGd_{0.1}Fe_{1.9}O_4$ annealed at 700° C in 5h

Fig. 3 shows the FTIR plots for $NiFe_2O_4$ and $NiGd_{0.1}Fe_{1.9}O_4$ samples. Formation of pure spinel structure has been confirmed by these plots of % Transmittance and wave number (400 cm^{-1} – 2000 cm^{-1}). It can be observed clearly that all the samples constitute two intrinsic frequency bands due to metal cations and oxygen bonds vibration. The band for lower wave number (υ_1 ~ 400 cm^{-1}) shows the octahedral metal cation and oxygen bond and high frequency band (υ_2 ~ 600 cm^{-1}) is for tetrahedral sub-lattice and oxygen ions bond. One more thing could also be observed that due to substitution of Gd^{3+} in nickel ferrites the frequency bands are shifting to higher frequency side that also confirms the substitution of Gd^{3+} at octahedral sites [13].

The magnetic isotherms were made at different temperatures from 88 K to 900 K (fig. 4). A common feature of the curves is that the magnetization approaches to saturation above ~ 2.5 kOe and with further increasing magnetic field a slow increase of the magnetization is observed. This high-field susceptibility is usually observed in Ferro/ferrimagnetic ultrafine particles which can be explained by the effect of canted or disordered spins at the particle surface. The obtained results are characteristic for superparamagnetic particles with blocking temperature above room temperature. The spontaneous magnetization values (M_{sp}) is determined by extrapolating the high-field linear part of the magnetization curve to zero field. The derived spontaneous magnetization values of the two samples are plotted as a function of temperature and are shown in Fig. 5. The spontaneous magnetization at zero Kelvin $M_{sp}(0)$ was estimated by extrapolation of the graphical plot of M_{sp} against T^{α} to $T = 0$ according to a modified Bloch law [14].

$$M_s(T) = M_s(0)[1 - BT^{\alpha}] \qquad (1)$$

where B is the Bloch's constant and α the Bloch exponent. The values of M_{sp} at 300 K, T_C and extrapolated $M_{sp}(0)$ of $NiFe_2O_4$ and $NiGd_{0.1}Fe_{1.9}O_4$ annealed 700° C in 5 h are listed in Table 2.

From the $M_{sp}(T)$ curves, the Curie temperature T_C were deduced as temperature where M_{sp} reduce to zero. It is seen that the magnetic parameters M_{sp} and T_C decrease with rare earth doping (Table 2). The distribution of cations in the spinel structure decides the magnitude of the exchange interactions between the magnetic moments at A and B sites, and therefore decide the values of Curie temperature. Gd^{3+} ions prefer to occupying the octahedral site which have larger size (Table 1). Because doping causes a decrease in B sublattice magnetization and hence the total magnetization. On the other hand, the reduction of M_{sp} in Gd doped sample suggests that even though Gd^{3+} ions carry magnetic moment due to the 4f electrons, they are not magnetically ordered. This can be explained due to the fact that the 4f shell locates closer to the nucleus of Gd^{3+} ion and cannot interact with surrounding Fe^{+3} ions. Beside, the particles size effect is also a factor responsible for the lower M_{sp} of the samples. Due to the lack of magnetic coordination numbers, magnetic ions in the surface region may not be aligned in parallel with the magnetization in the core volume of a particle which results in a decrease of the total magnetization. A core-shell model for a particle is usually used to estimate the magnetization reduction in a nanoparticle compared to the bulk value as $M_{sp} = M_{sp}^{bulk}[(D/2\text{-}t)/(D/2)]^3$ [15] where t is the thickness of the magnetic disorder layer and D is the diameter of the particle. Taking the mean particle size D_{XRD} as determined via XRD patterns for the samples, the average shell thickness t was calculated according to this expression and listed in Table 2.

Table 2. M_{sp} at 0 K (Bloch's function) and 300 K, T_C and t of $NiFe_2O_4$ and $NiGd_{0.1}Fe_{1.9}O_4$ annealed 700° C in 5 h.

Samples	$M_{sp}(0)$ (emu/g)	$M_{sp}(300)$ (emu/g)	T_c (K)	t *(nm)*
$NiFe_2O_4$	39.73	34.67	870	0.89
Ni-$Gd_{0.1}$	22.61	19.1	800	0.67

We now consider the variation of Curie temperature caused by size reduction and doping effect. With $NiFe_2O_4$ sample, T_C value equals to the value of the bulk sample (T_C = 860 K [16]). It is known that Curie temperature of a ferromagnetic sample reduces as its volume decreases to nanoscale. This observation indicates that the size reduction effect is not significant in the length scale of ~ 18 nm for nanosized nickel ferrite. The decreases in T_C of doped samples is firstly due to the replacement of Fe^{3+} by Gd^{3+} in the octahedral sublattice which leads to the decrease in the net magnetization and intra- and intersublattice exchange interaction J_{BB} and J_{AB}. The decrease in the effective field acting on the magnetic ions in the octahedral sites is responsible for the more rapid decline of the magnetization of the octahedral sublattice.

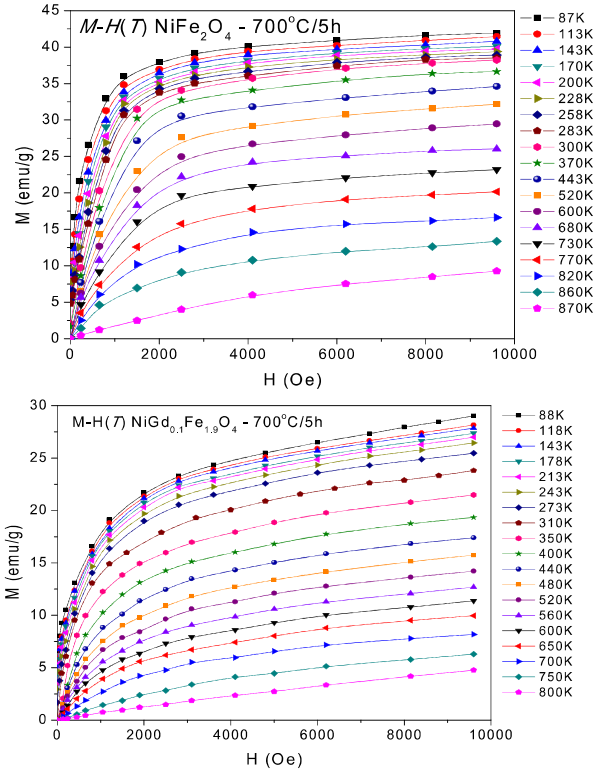

Fig. 4. Magnetic isotherm curves (M-H) measured at 87 K to 900 K for the samples $NiFe_2O_4$ and $NiGd_{0.1}Fe_{1.9}O_4$

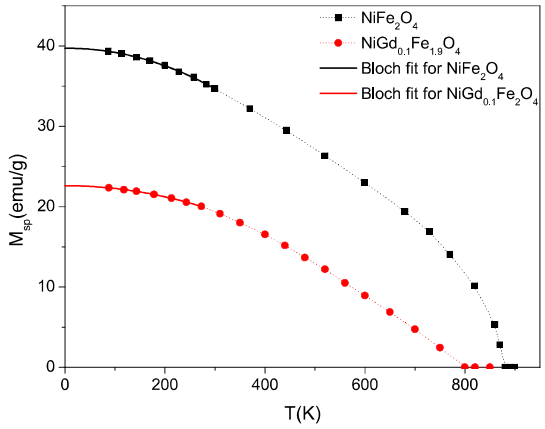

Fig. 5. Spontaneous magnetization M_{sp} as function of temperature for the samples $NiFe_2O_4$ and $NiGd_{0.1}Fe_{1.9}O_4$. The solid line are the fit curves according to Bloch's function.

4. Conclusion

$NiFe_2O_4$ and $NiGd_{0.1}Fe_{1.9}O_4$ spinel nanoparticles were obtained by using a modified citrate precursor technique. The results show that the substituted samples favorably form in single–phase at low annealing temperature (700° C in 5h). The samples have the cubic spinel structure at room temperature with the lattice constant *a* slightly decreases with doping Gd content. The particle size of the samples is significantly reduced by Gd substitution. The Rietveld refinement results indicate that Gd ions locate exclusively in octahedral site while nickel ions and iron ions for the most part locates in octahedral sites and a small amount of them are in tetrahedral sites. The magnetic moment values of the samples in the ground state were found. The influence of Gd^{3+} substitution for Fe^{3+} on the magnetic parameters of the samples including the spontaneous magnetization (M_{sp}), Curie temperature (T_C) were studied and compared with that of bulk materials. The changes in magnetic properties of the samples with Gd concentrations are explained via the change of interaction between the magnetic moments of magnetic cations in octahedral sites and tetrahedral sites. The magnetic measurements suggest remarkable influences of the particle size, interparticle interaction and cation distribution effects on their magnetic behavior.

Acknowledgments

This research is funded by the Hanoi University of Science and Technology (HUST) under project number T2016-PC-127.

References

[1]. R.K. Kotnala and Jyoti Shah, Handbook of Magnetic Materials (2015) 301-305.

[2]. C.N. Chinnasamy, A. Narayanasamy, N. Ponpandian, K. Chattopadhyay, K. Shonoda, B. Jeydefan, K. Tohji, K. Nakatsuka,T. Furubayashi, I. Nakatan, Phys. Rev. B 63 (2001) 184108.

[3]. Anju Ahlawat, V.G. Sathe n, V.R. Reddy, Ajay Gupta, Journal of Magnetism and Magnetic Materials 323 (2011), 2049-2054.

[4]. N. Rezlescu, E. Rezlescu, Solid State Commun. 88 (1993) 139.

[5]. K.K. Bharathi, JA Chelvane, G Markandeyulu, Journal of Magnetism and Magnetic Materials 321 (22), 3677-3680

[6]. K. Kamala Bharathi, K. Balamurugan, P. N. Santhosh, M. Pattabiraman, and G. Markandeyulu, Phys. Rev. B 77, (2008) 172401.

[7]. JP Singh, G Dixit, RC Srivastava, HM Agrawal, K Asokan, Journal of Physics D: Applied Physics 44 (43), 435306

[8]. Erum Pervaiz, I.H. Gul, Journal of Magnetism and Magnetic Materials 349 (2014) 27–34.

[9]. Gagan Dixit et al., Journal of Magnetism and Magnetic Materials 345, (2013) 65.

[10]. J. Rodriguez-Carvajal, Phys. B 192, 55 (1993).

[11]. L. B. McCusker, R. B. Von Dreele, D. E. Cox, D. Louër, and P. Scardi, J. Appl. Crystallogr. 32, (1999) 36.

[12]. T.D.H. To Thanh Loan, Nguyen Phuc Duong, Nguyen Kim Thanh, Luong Ngoc Anh, Tran Thi Viet Nga, J. Nanosci. Nanotechnol. 16, (2016) 7973.

[13]. R.D. Waldron, Phys. Rev. 99 (1955) 1727e1735.

[14]. P.V. Hendriksen, S. Linderoth, P.-A. Lindgård, J. Magn. Magn. Mater. 104–107 (1992) 1577–1579.

[15]. J. P. Chen, C. M. Sorensen, K.J.Klabunde, G.C.Hadjipanayis, E.Devlin, A.Kostikas, *Physical Review B*, 54 (1996), pp. 9288-9296.

[16]. B.D. Cullity, Introduction to Magnetic Materials, Addinson Wesley, New York, (1972).